

## PHOTOVOLTAIC PROPERTIES OF THE CdS/CdTe HETEROJUNCTION SOLAR CELLS BEFORE AND AFTER PROTON IRRADIATION

M. RADU<sup>a</sup>, V. GHENESCU<sup>b</sup>, I. STAN<sup>a,b</sup>, L. ION<sup>a</sup>, C. BESLEAGA<sup>a</sup>,  
A. NICOLAEV<sup>a</sup>, T.L. MITRAN<sup>a</sup>, C. TAZLAOANU<sup>a</sup>, A. RADU<sup>a</sup>, O. PORUMB<sup>a</sup>,  
M. GHENESCU<sup>b</sup>, M.M. GUGIU<sup>c</sup>, S. ANTOHE<sup>a\*</sup>

<sup>a</sup>*Department of Solid State Physics, University of Bucharest, 077125, Magurele-Ilfov, Atomistilor 405, Romania*

<sup>b</sup>*Institute for Space Sciences, 077125, Magurele-Ilfov, Atomistilor 409, Romania*

<sup>c</sup>*"Horia Hulubei" National Institute of Physics and Nuclear Engineering - IFIN HH, 077125, Magurele-Ilfov, Atomistilor 407, Romania*

In this work we report the experimental results of high-energy proton irradiations of 3 MeV and fluency of  $3 \times 10^{14}$  protons/cm<sup>2</sup> on CdS/CdTe heterojunction solar cells. The photovoltaic cells were developed on ITO coated optical glass substrates, by conventional thermal vacuum evaporation technique. The CdS/CdTe is given a post deposition CdCl<sub>2</sub> heat treatment which enables grain enhancement, reduces the defect density in the films, promotes the interdiffusion of the CdTe and CdS layers and thereby improves solar cell efficiency. The effects of irradiation were studied by investigating the changes in the electrical and optical properties of the cells. It was found that proton irradiation in the above mentioned conditions results mainly in the introduction of defects at the CdS/CdTe interface. From the I-V characteristics in fourth quadrant, at illumination in A.M. 1.5 conditions, measured before and after proton irradiation, the typical parameters as photoelement (short-circuit current, open-circuit voltage, fill factor, power conversion efficiency), were determined, before and after proton irradiation.

(Received July 25, 2011; accepted August 10, 2011)

*Keywords:* Photovoltaic cells; CdS/CdTe; CdCl<sub>2</sub> treatment; Space applications

### 1. Introduction

Polycrystalline CdTe thin film solar cells have shown long-term stable performance [1] and high efficiency up to 16.5% under AM1.5 illumination [2-8]. The solar cells based on thin films such as CdS, CdTe are promising candidates for the economically viable large scale terrestrial production of electricity in the near future. The critical stages in device fabrication is the treatment of the CdTe film, with CdCl<sub>2</sub>, a process that is essential in the production of high-efficiency cells. Besides their capability to open new terrestrial market segments, they are considered as competitive candidates for future thin film space power generators compared to traditional crystalline solar cells. Space applications require low mass, low specific volume, low cost and mechanical reliability at high temperatures and vigorous vibrations. One of the most important requirements for the space application is radiation hardness, because it determines the useful lifetime of satellites.

Here we approach the study of the effects of proton irradiation on the performance of photovoltaic cells based on polycrystalline CdS/CdTe thin layers. CdS/CdTe thin film photovoltaic cells developed in our laboratory were irradiated with 3 MeV energy protons to fluencies of  $3 \times 10^{14}$  protons/cm<sup>2</sup> through the back side of solar cells to determine their radiation tolerance. The

---

\* Corresponding author: [santohe@solid.fizica.unibuc.ro](mailto:santohe@solid.fizica.unibuc.ro)

paper is organized as follows: details concerning the experimental procedures we have used are given in section 2. The results are discussed in section 3 and the main conclusions are summarized in the final section.

## 2. Experimental details

In the present work we report on the fabrication and characterization of a CdS/CdTe photovoltaic cells. The solar cells structures were grown in a „superstrate configuration” onto the ITO coated optical glass substrate. CdS layer of  $\sim 1 \mu\text{m}$  was prepared by thermal vacuum evaporation. CdS powder (Aldrich) was grown at a pressure of  $3.2 \times 10^{-4}$  mbar from a quartz container heated to  $740^\circ\text{C}$ , the substrate temperature being maintained at  $250^\circ\text{C}$ . To prevent the sputtering of the powder during the sublimation process, the evaporator was covered with a quartz-wool plug. To improve the structural quality of the thin layers, they were thermally treated in vacuum at  $350^\circ\text{C}$  for 15 min. [9,11]. The CdTe layer of  $\sim 2.5 \mu\text{m}$  was subsequently grown in the same chamber by evaporation of CdTe source material. CdTe powder (Aldrich) was vacuum sublimated from a quartz evaporated heated to  $600^\circ\text{C}$ , with the substrate at  $250^\circ\text{C}$  and the whole structure was thermally treated in vacuum at  $350^\circ\text{C}$  for 18 min. [12]. After thermally treated, the ITO/CdS/CdTe structures were also subjected to chemical treatment.  $\text{CdCl}_2$  treatment is applied after deposition of the CdTe absorber layer and prior to the application of the back contact. The  $\text{CdCl}_2$  powder was vacuum sublimated at a pressure of  $10^{-5}$  Torr from a quartz container, heated to  $700^\circ\text{C}$  for 5 minutes. Also, to prevent the sputtering of the powder during evaporation, the container was covered with a quartz-wool plug and the distance between itself and structure was 5 cm, the substrate temperature being maintained at  $125^\circ\text{C}$ . The chemical treatment of the structures with  $\text{CdCl}_2$  is crucial step for obtaining photovoltaic activity [13].

After that, the back contact was evaporated on top of the CdTe layer, to complete the cell structure, consisting of 50 nm copper layer and 100 nm gold layer. The back contact generally includes two layers: the primary layer is a heavily doped layer that makes a low-loss electrical contact to the CdTe; and the secondary contact is metal that carries the current laterally. The primary layer employs Cu, because the Cu diffuses into the CdTe and produces a heavily doped p-layer. This helps to reduce barrier height between CdTe and back contact. After the Cu electrode deposition an annealing treatment in vacuum at  $200^\circ\text{C}$  for 15 minutes was applied. Electrical contacts to the electrodes were secured by silver paste. The active area of each cell was  $0.4 \text{ cm}^2$ .

The ITO/CdS/CdTe/Cu/Au solar cells treated in  $\text{CdCl}_2$  were subjected to irradiation from the backside with protons supplied by an accelerator, the proton beam being directed along the normal to the surface of the samples. Irradiation was carried out in an evacuated chamber, at ambient temperature, with 3 MeV protons to a fluency of  $3 \times 10^{14}$  protons/ $\text{cm}^2$ . During irradiation the thermal effect was negligible.

All the devices fabricated were subjected to both dark and light current-voltage (I-V) measurements. Dark I-V measurements were done covering the devices with a black paper and light I-V measurements were done at AM1.5 solar spectrum which was achieved using Newport-Oriel 150 solar simulator equipped with an Hg-Xe high pressure lamp. The current was measured using a 2400 Keithley Source Meter. The range of the sweeping voltage across the devices is set using a labview program which is connected with the source meter. The specific software was used to collect the I-V data. I-V curve is plotted and displayed immediately on the monitor, when the measurement is finished and an I-V curve is obtained. The measure I-V characteristic,  $100 \text{ mW}/\text{cm}^2$  density of light power was used.

For action spectra and external quantum efficiency (EQE) measurements, an experimental setup containing a Newport Oriel monochromator, controlled by a computer, was used. Optical properties of the CdS and CdTe films were characterized by performing transmittance and absorption measurements. The data were recorded at room temperature, with a Perkin-Elmer Lambda 35 spectrometer.

### 3. Results

#### 3.1. Current-Voltage characteristics in the dark

The current-voltage (I-V) characteristics of an ITO/CdS/CdTe/Cu/Au solar cells treated in CdCl<sub>2</sub> measured in dark, before and after irradiation, at room temperature, in both forward and reverse bias conditions, are shown in figure 1(a, b). As expected, the forward bias conditions correspond to positive voltage on the gold electrode with respect to the ITO front contact electrode. A thorough analysis of the dark I-V characteristics of the cell, starting from the modified Shockley equation [14], allows for a characterization of CdS/CdTe interface, responsible for both electric and photovoltaic behavior of the cell.

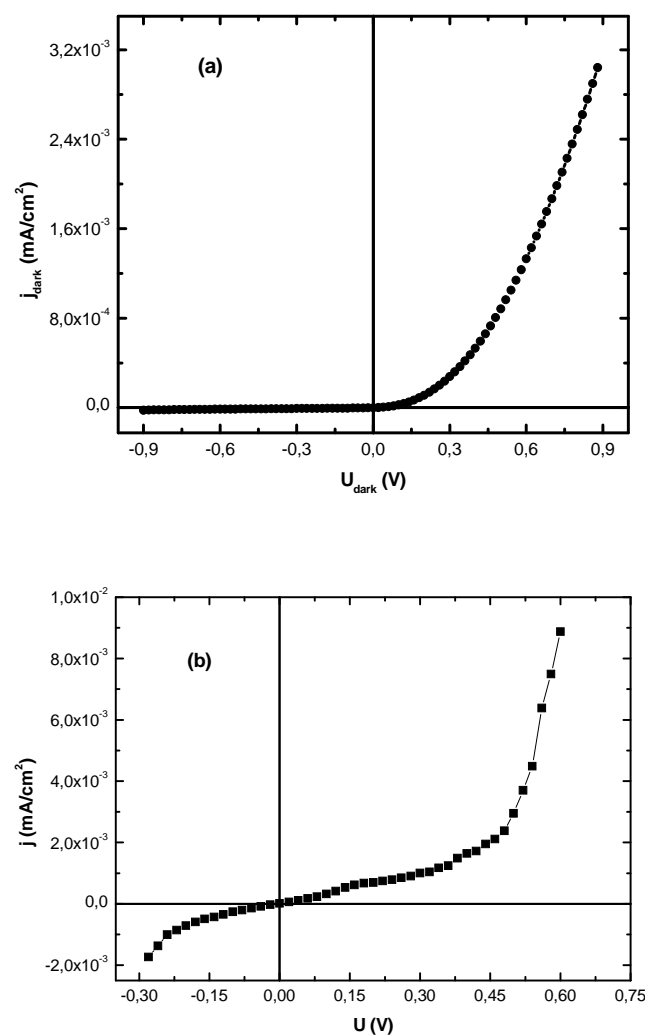


Fig. 1. I-V characteristics of ITO/CdS/CdTe/Cu/Au cell in dark (a) before and (b) after irradiation.

The modified Shockley equation is given by:

$$I = I_o \left\{ \exp \left[ \beta (V - IR_s) \right] - 1 \right\} + \frac{V - IR_s}{R_{sh}} \quad (1)$$

where:  $I_0$  is the reverse saturation current,  $R_s$  – the series resistance and  $R_{sh}$  – the shunt resistance. Here  $\beta = q/nkT$ , where  $q$  is the electronic charge,  $n$  – the diode quality factor,  $k$  – the Boltzmann constant, and  $T$  – the absolute temperature. The differential resistance of the cell is given by:

$$R_o = \frac{dV}{dI} = R_s + \frac{1}{\left\{ \beta I_o \exp[\beta(V - IR_s)] + \frac{1}{R_{sh}} \right\}} \quad (2)$$

At high voltages, in forward bias, eq. (1) becomes  $I = I_o \exp[\beta(V - IR_s)]$  and then Eq. (2) simplifies to:

$$R_o \cong R_s + \frac{1}{\beta I} \quad (3)$$

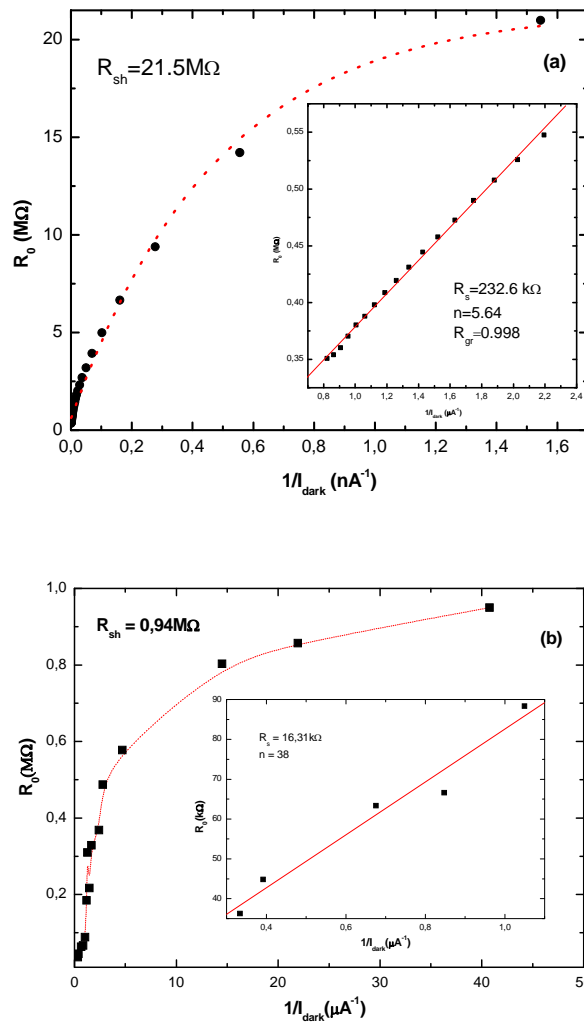


Fig. 2. Dependence of the differential resistance of ITO/CdS/CdTe/Cu/Au cell on the reciprocal of the current at forward bias, (a) before and (b) after irradiation

Thus, in the range of high voltages of  $R_o$  vs.  $1/I_{dark}$  plot, before and after irradiation, shown in figure 2 (a, b), the values for  $R_s$  and  $n$  parameters can be extracted. At low voltages, where the

current flowing through  $R_{sh}$  becomes important, eq. (2) becomes  $R_o \cong R_s + R_{sh}$ . Since  $R_s \ll R_{sh}$ , it follows that  $R_o$  is essentially  $R_{sh}$  at low voltages.

Further on, in order to get more accurately the values of  $I_0$  and  $n$ , eq. (1) has been transformed as:

$$I - \frac{Y}{R_{sh}} = I_0 [\exp(\beta Y)] \quad (4)$$

where:  $I - \frac{Y}{R_{sh}}$  is the current flowing through the barrier and  $Y = V - I R_s$ , the real voltage drop across it, respectively.

The plot of  $\ln\left(I - \frac{Y}{R_{sh}}\right)$  vs.  $Y$  is shown in figure 3. After removing the effects of series and shunt resistances, the linear part in the plot was extended considerably, increasing the accuracy in the determination of  $I_0$  and  $n$  values.

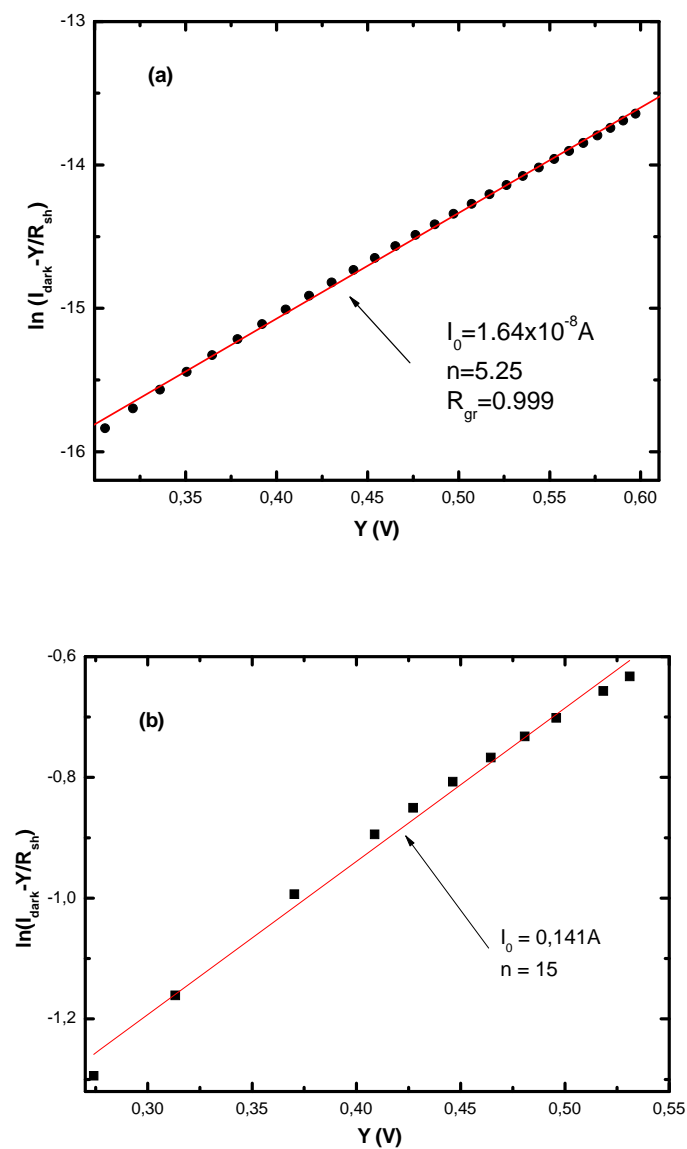


Fig. 3. The  $\ln(I - Y/R_{sh})$  vs  $f(Y)$  characteristics for ITO/CdS/CdTe/Cu/Au cell (a) before and (b) after irradiation

Moreover, the values for series and shunt resistances, the reverse saturation current and the quality diode factor were calculated and will be shown in table 1.

Table 1: Parameters characterizing a photovoltaic cells

Parameter	As grown	Irradiated
$R_s$ ( $k\Omega$ )	232.6	16.31
$R_{sh}$ ( $M\Omega$ )	21.5	0.94
$I_0$ (A)	$1.64 \times 10^{-8}$	0.141
n	5.25	15

### 3.2. Current-Voltage characteristics, at illumination in fourth quadrant

Typical I-V characteristics in the fourth quadrant, under AM1.5 conditions, measured before and after irradiation for ITO/CdS/CdTe/Cu/Au photovoltaic cells are shown in figure 4.

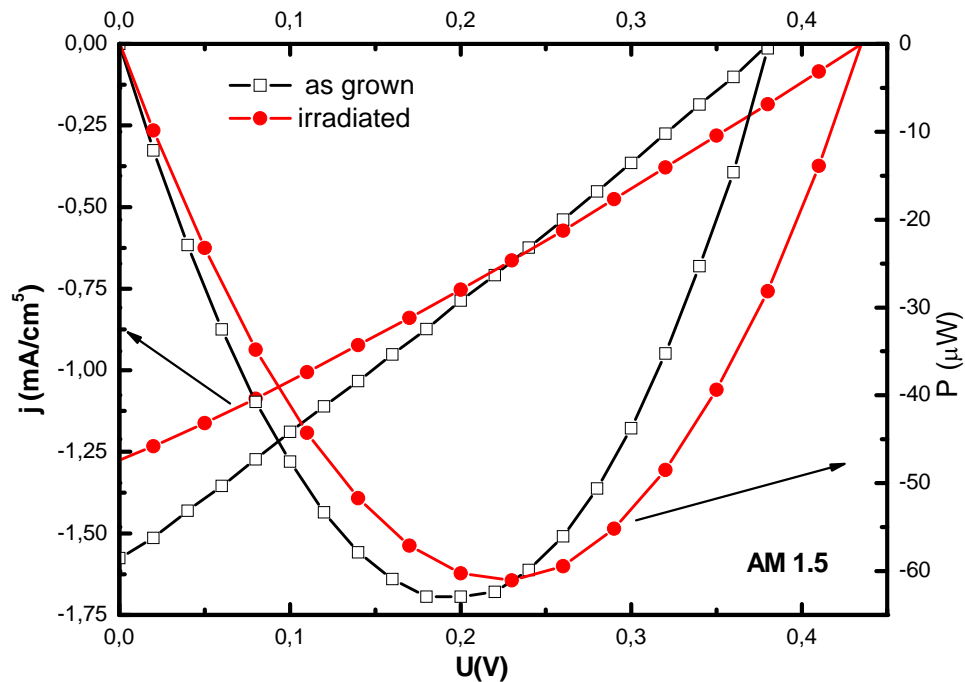


Fig. 4. I-V characteristics of the ITO/CdS/CdTe/Cu/Au device measured under AM 1.5 illuminations, before and irradiation

The main parameters of the photovoltaic cells, derived from I-V measurements before and after irradiation, are shown in table 2.

Table 2: *I-V* parameters of the cell before and after irradiation

Parameter	As grown	Irradiated
$V_{OC}$ (mV)	380	430
$J_{sc}$ (mA/cm <sup>2</sup> )	1.57	1.28
FF (%)	27.7	26.3
$\eta$ (%)	0.16	0.14

### 3.3. Spectral characterization

Absorption at small wavelength is expected to be large, and therefore photons of high energy are absorbed in the CdS region (provided  $\lambda \geq E_{g-CdS}$ ) or very near the CdS/CdTe interface. Longer wavelengths are absorbed closer to the back contact, as the photon energy approaches the CdTe band gap.

Figure 5 shows the spectral dependence of the normalized external quantum efficiency (*EQE*) recorded for one of the *ITO/CdS/CdTe/Cu/Au* cell both before and after irradiation with 3 MeV protons to fluencies of  $3 \times 10^{14}$  protons/cm<sup>2</sup>. The spectral dependence of the normalized external quantum efficiency (*EQE*) demonstrates significant loss of photon yield for wavelengths above the CdS band gap. However, since the CdS layer is responsible for collecting the electrons generated from photon absorption within the CdTe region, degradation of this layer may influence device performance. After irradiation, the quantum efficiency spectrum was not significantly changed, *EQE* values decrease for photon energies in the range corresponding to absorption in CdTe, (i.e., 1.48 eV, 2.5 eV), and increase for photon energies in the range corresponding to fundamental absorption in CdS layer proving that the space-charge region is now more extended into CdS layer.

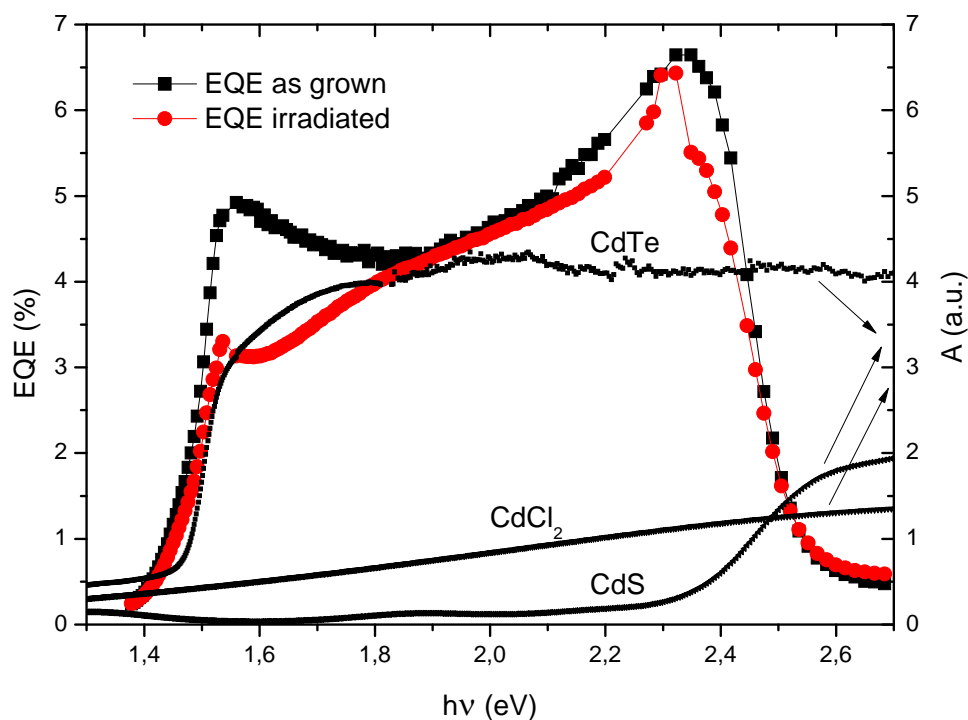


Fig. 5. Normalized EQE spectrum before (black) and after (red) irradiation with 3 MeV protons for ITO/CdS/CdTe/Cu/Au structure and absorption spectra of constitutive CdTe, CdS and CdCl<sub>2</sub> (grey line) layers of the cell

EQE decreasing in the spectral range corresponding to photo-generation of free carriers in CdTe can be related to the decrease of their life time due to irradiation damage.

In the same figure the energy derivative of EQE is also plotted against the incident photon energy. The latter graph shows a sharp peak at 1.47 eV, before and after irradiation, corresponding to the inflecting point of the spectral response, which is normally taken as the energy band gap of CdTe. A more accurate value for the band gap can be determined from a plot of quantum efficiency  $(EQE \cdot E)^2$  against the incident photon energy  $E$ . This is due to the fact that for sub-band gap photon energies EQE is proportional to the material optical absorption coefficient. The inset of figure 6 shows the straight-line plot of  $(EQE \cdot E)^2$  against  $E$  whose horizontal intercept measures a band gap value of 1.481 eV and 1.475 eV for CdTe, before and after proton irradiation, respectively.

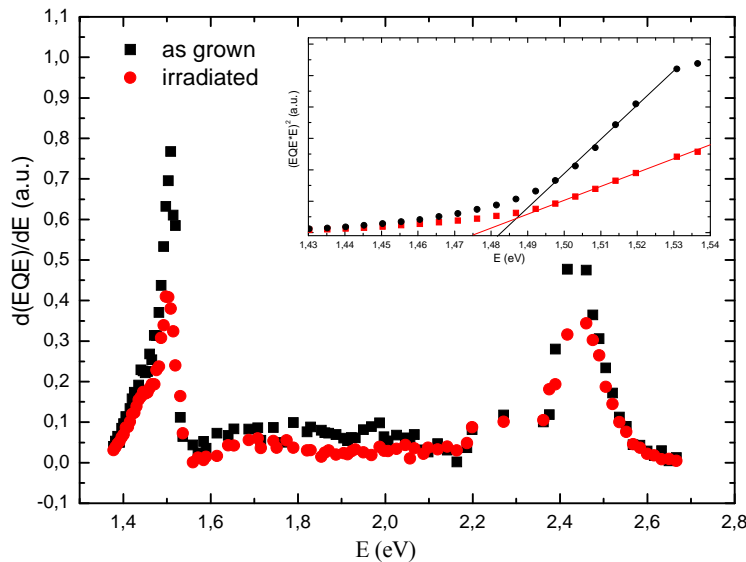


Fig. 6. The energy derivative of EQE against the incident photon energy. The energy band gap for CdTe is obtained from the inset plot

In order to get a more detailed image of the proton irradiation damage in our cell, the software package SRIM-2008 [15] was used in full collision cascade mode. At 3 MeV energy most of these protons are transmitted, but a significant damage can be observed at the CdS/CdTe interface, where most of the vacancies are produced in CdTe layer and inter-diffusion of S and Te recoil atoms occurs [16].

#### 4. Conclusions

The ITO/CdS/CdTe/Cu/Au photovoltaic cells were prepared and characterized, investigating the effect of proton irradiation on their performances.

The I-V characteristics in dark are nonlinear, highly asymmetric, and based on the data from forward bias a model was developed to extract with accuracy the electrical parameters characterizing the CdS/CdTe heterojunctions, before and after proton irradiation. From the I-V characteristics in fourth quadrant, at illumination in A.M. 1.5 conditions, measured before and after proton irradiation, the typical parameters as photoelement (short-circuit current, open-circuit voltage, fill factor, power conversion efficiency), were determined. The influence of the irradiation

with 3 MeV protons ( $3 \times 10^{14}$  protons/cm<sup>2</sup>) on the spectral performance of ITO/CdS/CdTe/Cu/Au photovoltaic cells was investigated. At this energy, most of the incident protons are transmitted and significant radiation damage occurs at CdS/CdTe interface.

The CdS/CdTe photovoltaic structure is given a post deposition CdCl<sub>2</sub> heat treatment which enables grain enhancement, reduces the defect density in the films, promotes the interdiffusion of the CdTe and CdS layers and thereby improves solar cell efficiency. Moreover, the CdCl<sub>2</sub> heat treatment improves the CdS/CdTe junction by enhancing the inter-diffusion between the semiconductors leading to the formation of a alloyed at interface. The CdCl<sub>2</sub> treatment lead to an improvement of stability of the performances of the CdS/CdTe heterojunction against the proton irradiation such as results from the smaller differences between the EQE spectra before and after proton irradiation.

### Acknowledgements

This work was partially supported by the project POSDRU 107/1.5/S/80765 .

### References

- [1] D.L. Batzner, A. Romeo, H. Zogg, R. Wendt, A.N. Tiwari, *Thin Solid Film* **387**, 151 (2001)
- [2] X. Wu, J.C. Keane, R.G. Dhere, C. DeHart, D.S. Albin, A. Duda, T.A. Gessert, S. Asher, D.H. Levi, P. Sheldon. In: Proc. 17th European Photovoltaic Solar Energy Conference, Munich, Germany, 995 (2001).
- [3] X. Wu, *Sol. Energy* **77**, 803-814 (2004)
- [4] I.M. Dharmadasa, J. Haigh, *J. Electrochem. Soc.* **153**, G47-G52 (2006)
- [5] I. Enculescu, M. Sima, M. Enculescu, M. Enache, L. Ion, S. Antohe, R. Neumann, *PHYSICA STATUS SOLIDI B-BASIC SOLID STATE PHYSICS* **244**(5), 1607 (2007)
- [6] S. Antohe, L. Ion, V. Ruxandra, *J. Appl. Phys.* **90**(12), 5928 (2001)
- [7] M. Ghenescu, L. Ion, I. Enculescu, C. Tazlaoanu, VA. Antohe, M. Sima, M. Enculescu, E. Matei, R. Neumann, O. Ghenescu, V Covlea, S. Antohe, *PHYSICA E-LOW-DIMENSIONAL SYSTEMS & NANOSTRUCTURES* **40**(7), 2485 (2008)
- [8] L. Ion, S. Antohe, M. Popescu, F. Scarlat, F. Sava, F. Ionescu, *J. Optoelectron. Adv. Mater.* **6**(1), 113 (2004)
- [9] Veta Ghenescu, L. Ion, M. Ghenescu, M. Rusu, M. Gugiu, G. Velisa, Oana Porumb, S. Antohe, *Optoelectron. Adv. Mater.-Rapid Comm.* **3**(10), 1023 (2009)
- [10] L. Ion, V. Ghenescu, S. Iftimie, V. A. Antohe, A. Radu, M. Gugiu, G. Velisa, O. Porumb, S. Antohe, *Optoelectron. Adv. Mater.-Rapid Comm.* **4**(8), 1114 (2010)
- [11] G. Bakiyaraj, N. Gopalakrishnan, R. Dhanasekaran, *Chal. Lett.* **8**(7), 419 (2011)
- [12] Rosemary Bazavan, Oana Ghenescu, M. Ghenescu, Dora Crisan, A. Radu, L. Ion, S. Antohe, *J. Optoelectron. Adv. Mater.* **10**(11) 3048 (2008)
- [13] A.Rios-Flores, J. L. Pena, V. Castro-Pena, O. Ares, R. Castro-Rodriguez, A. Basio, *Solar Energy*, **84**, 1020 (2010)
- [14] Antohe, S.; Ruxandra, V.; Tugulea, L.; Gheorghe, V.; Inascu, D.; *J. Phys. III France* **6**, 1133 (1996)
- [15] ] J. F. Zeigler, J.P. Biersack, U. Littmark, *The stopping and range og ions in solids*, Pergamon Press, New York, (1985)
- [16] L. Ion, I. Enculescu, Sorina Iftimie, Veta Ghenescu, C. Tazlaoanu, Cristina Besleaga, T.L. Mitran, V. A. Antohe, M.M. Gugiu, S. Antohe, *Chalc. Lett.* **7**(8), 521 (2010)